A Journal of the Gesellschaft Deutscher Chemiker

Angewandte International Edition GDCh Chemie

www.angewandte.org

Accepted Article

Title: Iodane-guided ortho C-H allylation

Authors: Alexandr Shafir, Wei W. Chen, Anton Cunillera, Dandan Chen, Sébastien Lethu, Albert López de Moragas, Jun Zhu, Miquel Solà, and Ana B. Cuenca

To be cited as: *Angew. Chem. Int. Ed.* 10.1002/anie.202009369

Link to VoR: https://doi.org/10.1002/anie.202009369

WILEY-VCH

10.1002/anie.202009369

WILEY-VCH

RESEARCH ARTICLE

Iodane-guided ortho C-H allylation

Wei W. Chen,[a,b] Anton Cunillera,[a] Dandan Chen,[c,d] Sébastien Lethu,[e] Albert López de Moragas,[b] Jun Zhu,[d] Miquel Solà,*[c] Ana B. Cuenca*[b] and Alexandr Shafir*[a]

[a] W. W. Chen, Dr. A. Cunillera, Dr. A. Shafir
Dept. of Biological Chemistry, Centro de Innovación en Química Avanzada (ORFEO-CINQA),
Institute of Advanced Chemistry of Catalonia (IQAC-CSIC)
c/Jordi Girona 18–26, 08034 Barcelona (Spain); alexandr.shafir@iqac.csic.es
[b] W. W. Chen, A. López de Moragas, Dr. A. B. Cuenca
Dept. of Organic and Pharmaceutical Chemistry, Institut Químic de Sarrià, Universitat Ramon Llull
Via Augusta 390, 08017 Barcelona (Spain), anabelen.cuenca@iqs.url.edu
[c] D. Chen, Prof. Dr. M. Solà
Institute of Computational Chemistry and Catalysis and Department of Chemistry
University of Girona, C/ M. Aurèlia Capmany, 69, 17003 Girona, Catalonia, Spain; miquel.sola@udg.edu
[d] D. Chen, Prof. Dr. Jun Zhu
State Key Laboratory of Physical Chemistry of Solid Surfaces and Collaborative Innovation Center of Chemistry for Energy Materials (iChEM), Fujian Provincial Key Laboratory of Theoretical and Computational Chemistry and Department of Chemistry, College of Chemistry and Chemical Engineering Xiamen University, Xiamen 361005 (China)
[e] Dr. S. Lethu
Institute of Chemical Research of Catalonia, BIST
Avda. Països Catalans 16, 43007 Tarragona, Spain

Abstract: A metal-free C-H allylation strategy is described to access diverse functionalized *ortho*-allyl-iodoarenes. The method employs hypervalent (diacetoxy)iodoarenes and proceeds through the iodane-guided "iodonio-Claisen" allyl transfer. The use of allylsilanes bearing electron-withdrawing functional groups unlocks the functionalization of a broad range of substrates, including electron-neutral and electron-poor rings. The resulting *ortho*-allylated iodoarenes are versatile building blocks, with examples of downstream transformation including a concise synthesis of the experimental antimitotic core of Dosabulin. DFT calculations shed additional light on the reaction mechanism, with notable aspects including the aromatic character of the transition state structure for the [3,3] sigmatropic rearrangement, as well as the highly stereo-convergent nature of the *trans* product formation.

State of the art. A great deal of effort has gone into the development of both the allyl-forming and allylation methodologies, including those leading to allylated arenes.[1] In particular, metal-catalyzed cross-coupling has been used to introduce the allylic fragment, either as a formal electrophilic,[2] or nucleophilic precursor, e.g. allyl-tin, -magnesium[3] or -boronate[4] species. Recently, powerful C-H allylation strategies have also been developed, particularly those based on the ligand-directed metal-catalyzed C-H activation.[5] In this report we present an alternative method for oxidative C(sp^2)-H allylation of iodoarenes based on the iodonio-Claisen concept. The mechanistic pillars of this reaction are rooted in the 1990's, when the groups of Ochiai and Norton showed that a reaction between simple λ^3-iodanes,[6] such as phenyliodine diacetate, and the propargyl(trimethyl)silane leads to the formation of a fleeting λ^3-(allenyl)(phenyl)iodonium product. This species rapidly undergoes a [3,3] sigmatropic rearrangement to give the *ortho*-propagyl-iodoarene (Scheme 1-A).[7] We recently showed this C-H alkylation process to be an excellent tool to access to a wide range of *ortho*-propargylated iodoarene cores.[8] Furthermore, over the last decade, a small number of teams, ours included, have developed a range of *ortho* C-H coupling reaction reactions, including those based on enols, phenols, and cyanoalkyl substrates,[9] with the reactivity later extended to *para*-selective C-H coupling.[10-12] Importantly, a 2012 study by J. Zhu and coworkers showed that while the C-H coupling of the allyl(trimethyl)silane, **1**, was feasible, this reaction was only applicable to certain very electron-rich λ^3-iodoarene cores,[13-15] largely failing even for the "neutral" iodoarene core of the parent ArI(OAc)$_2$ (Scheme 1, B).

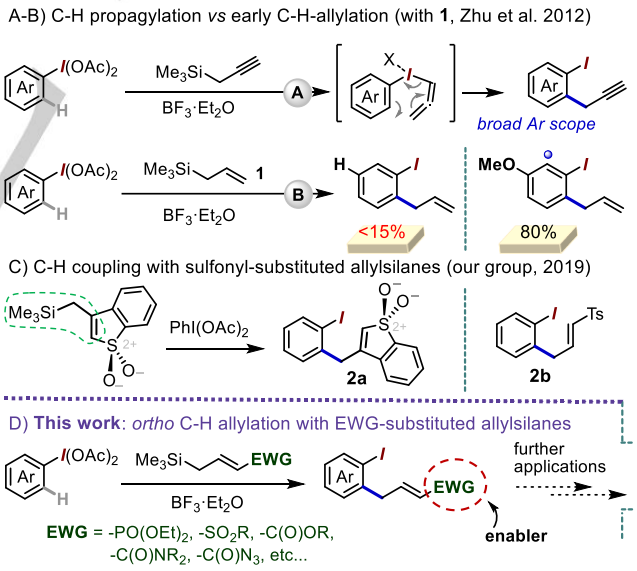

Scheme 1. Selected precedents in iodane-guided C-H coupling reactions.

In this context, our group reported a surprisingly efficient *ortho*-C-H coupling of the benzothiophene-*S*-dioxide reagent containing an imbedded allylsilane unit (prod. **2a**, Scheme 1, C); efficient reactivity was also observed for a tosyl-substituted allyltrimethylsilane (prod. **2b**).[11, 16] This suggested that perhaps equipping an allylsilane reagent with an electron-withdrawing group (EWG) could be the key to a broad-scope iodane-directed C-H allylation process. Prompted by this possibility, a method is

10.1002/anie.202009369

now presented to produce a diverse range of *ortho*-iodo-allylarenes *via* a C-H allylation process in which the allyl-bound EWG can not only act as a reaction booster, but will subsequently engage in a downstream functionalization, including those leading to potentially bioactive cores (Scheme 1, D).

Initial C-H allylation assays. Initially, the coupling of the phosphoryl-substituted allylsilane **3**, obtained by olefin cross-metathesis between **1** and the diethyl vinylphosphonate,[17] was tested with the *para*-Cl-λ^3-iodane **4**. When conducted in a CH_2Cl_2/CH_3CN solvent mixture, which has been found optimal in prior works,[13a,8,11] no intended *ortho*-allylarene **5** was detected in the absence of an acid activator (Table 1, entry 1). Gratifyingly, the addition of 1.2 equiv of $BF_3{\cdot}Et_2O$ allowed for the formation of phosphorylated allylarene **5** in 57% yield (NMR), with further improvements to 85% (74% isolated) achieved by raising the additive loading to 2.0 equiv. (see entries 2-4).[18] HOTf and TMSOTf could also be employed as acid activators (entries 5, 6). Incidentally, only trace amounts of the C-H coupling product were achieved using the unsubstituted allylsilane **1**.[19]

Table 1. Additive effect in the reaction between **3** and **4**.[a]

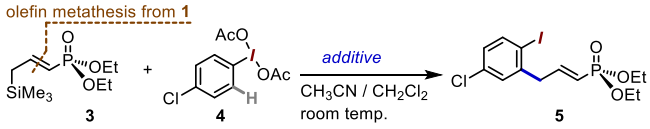

run	*additive*	% **5**[b]	run	*additive*	% **5**[b]
1	none	nd	4	3.0 eq $BF_3{\cdot}Et_2O$	79%
2	1.2 eq $BF_3{\cdot}Et_2O$	57%	5	1.2 eq HOTf	54%
3	2.0 eq $BF_3{\cdot}Et_2O$	85% (**74%**)[c]	6	1.2 eq TMSOTf	74%

[a] Using 0.2 mmol ArI(OAc)$_2$ and 0.24 mmol allylsilane **3** in 1.4 mL of solvent; [b] % ^{1}H-NMR yield using naphthalene as internal standard; [c] isolated yield.

Next, additional *trans*-allylsilanes were prepared by cross-metathesis, including the sulphones **6** and **7**-Me, as well as the acryloyl ester **8** and amides **9** and **10** (Table 2). These were then tested in C-H allylation of both the chloro-substituted λ^3-iodane **4** and the parent λ^3-PhI(OAc)$_2$. Gratifyingly, not only **3**, but also **6**, **7**, and **8** afforded the target *ortho*-allylated products in synthetically attractive yields (prods. **11**-**17**), with no significant efficiency differences within the *p*-H *vs* *p*-Cl substrate pairs (Table 2). All products were obtained as *trans*-olefins, with only the ester **16** showing small amounts of the *cis* isomer. Electronic differentiation between iodoarene cores did manifest itself for the *N*,*N*-dimethylacrylamide **9**, for which the EWG = $CONR_2$ has a Hammett σ_p <0.36, making it the least withdrawing substituent in the series at hand.[20] This lower Hammett parameter appears to correlate with a less efficient coupling between **9** and the *p*-Cl substrate **4** (<20% yield, prod. **18**). Nevertheless, switching from **4** to PhI(OAc)$_2$ gave the C-H allylated species **19** in 77% yields. Hence, while the reactivity of **9** could be considered as "borderline", its ability to couple with an electron-neutral aryliodane reflects a performance still far superior to that of the non-substituted allylsilane **1** (e.g. see Scheme 1B). Finally, despite the poor performance of the acrylamide **10**, its use with PhI(OAc)$_2$ at this stage did afford a 23% yield of the *ortho*-allylated target. While this shortcoming could be attributed to the known iodane-promoted Hoffmann-type rearrangement of a primary amide,[21] we have so far not been able to detect the product of such process.

Table 2. C-H coupling with additional allylsilane substrates.[a]

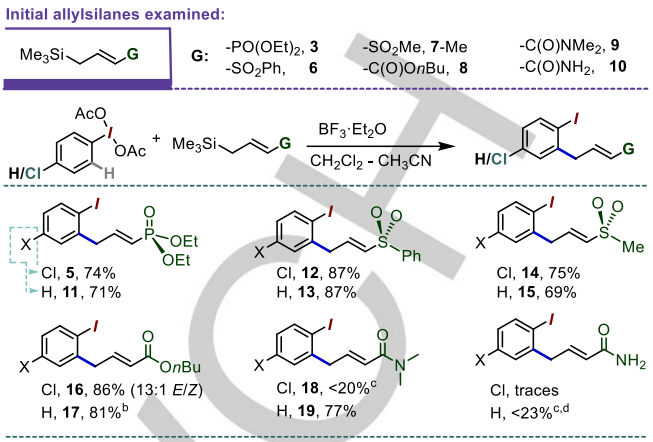

[a] Using ArI(OAc)$_2$ (1 equiv) and allylsilane (1.2 equiv) with 1.5-4.0 equiv of $BF_3{\cdot}Et_2O$; [b] Only *E* isolated; [c] % by NMR (see ESI); [d] -78 °C -> room temp

C-H allylation: a deeper look at the scope. Next, the study was amplified to a wider range of iodoarenes (Table 3). We were particularly satisfied with the efficient reactions of the electronically neutral and deactivated *p*-, *o*-, and *m*-halogenated substrates (Table 3, prod. **20**-**25**), as well as those bearing the *para*- -CO_2Me, -CF_3, -OCF_3 and -Ph groups (prod. **26**-**30**). The protocol was also applicable to iodonaphthalenes, including the 2-iodo-4-bromo derivative (prod. **31**-**37**), and to the λ^3-iodanes derived from the 1- and 2-iodothiophenes (prod. **38**, **39**). Despite the presence of two differentiated *ortho* sites in the 2-iodonapthalene and 3-iodothiophene precursors, the allylarenes **36**, **37**, and **39** each formed as a single regioisomer. In addition, as has been observed in related processes (e.g. ref. 8), the use of the *p*-OMe iodoarene substrate led to a partial formation of the des-iodo *ipso*-allylated product. The use of the 1,4'-bis-(λ^3-diacetoxyiodo)biphenyl resulted in a 45% yield of the doubly C-H-functionalized derivative **40**. As a more advanced substrate, the λ^3-form of the Boc-protected 4-iodophenylalanine, **41**, was transformed into the *N*-deprotected **42** (91%) in the presence of TMSOTf. Finally, the *in situ* formation of an estrone-derived λ^3-iodane gave the formation of **43** as a ~1:1 regioisomeric mixture. The target scope was further amplified through a divergent strategy based on the acyl chloride **44**, obtained from acryloyl chloride by olefin metathesis.[22] In an initial test, **44** was converted to the amide **45** (Table 3, lower half), paving the way for the formation of the morpholine-containing C-H allylarene **46**. Importantly, the modularity of this approach allowed for a rapid generation of additional amide-based allylarenes **47**, **48** or the proline-substituted **49** (Table 3, lower part). At this stage, the coupling of these amide-substituted allylsilanes with electronically deactivated iodoarene cores proved inefficient (see **47´**, 7%), but this will be revisited in the final section (*vide infra*). The acyl chloride **44** was also converted to allylsilanes terminated by the –CO_2H and –CON_3 groups, both of which show reactivity profiles that are broader than those of their amide analogues, as reflected in the C-H coupling with both activated and deactivated aryliodanes (see products **50**-**53**). Finally, an allylsilane obtained by quenching **44** with NHMe(OMe) allowed for the synthesis of a small family of the Weinreb amides **54**-**56**.

10.1002/anie.202009369

WILEY-VCH

RESEARCH ARTICLE

Table 3. Examples of functionalized *ortho*-iodo allylarenes obtained by the iodane-guided C-H coupling.[a]

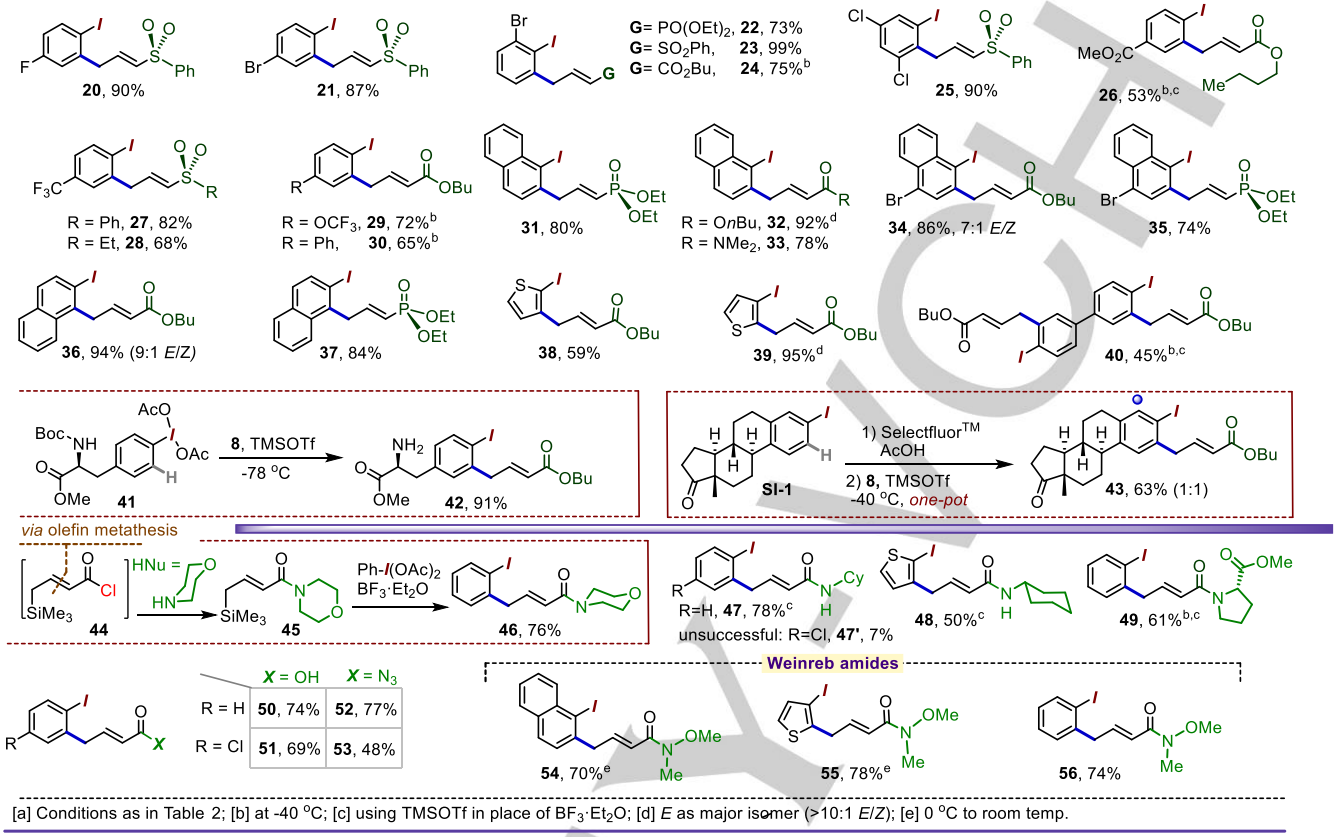

[a] Conditions as in Table 2; [b] at -40 °C; [c] using TMSOTf in place of $BF_3{\cdot}Et_2O$; [d] *E* as major isomer (>10:1 *E*/*Z*); [e] 0 °C to room temp.

Mechanistic aspects. To gain better understanding of the underlying mechanistic phenomena, a combined computational and experimental study was undertaken. The density functional theory (DFT) computations were performed at the M06-2X/aug-cc-pVTZ(-PP)//M06-2X/def2-SVP level. The entire reaction profile was elucidated for allylic sulfone precursor **7**-Me (Figure 1, **G** = SO_2Me); in addition, individual stages were studied for the systems with EWG = $PO(OEt)_2$, $CONMe_2$, and COOMe. Based on the group's earlier mechanistic studies,[18] the BF_3-activated adduct PhI(OAc)(OAc·BF_3) was employed as the reacting λ^3-iodane species. The reaction begins with an initial iodine(III)-olefin interaction between this adduct and the allylsilane **7**-Me, which weakens the C-Si bond (via the β-Si effect) and culminates with an abstraction of the Me_3Si group by one of the fluorides ceded by the newly formed F_3B-OAc^- anion (see Figure 1 and Figure S1 for more details). This process ($\Delta G^{\ddagger}$ = 14.5 kcal·mol^{-1}), results in a new I-C σ-bond (**Int0**) and the release of Me_3SiF, the latter observed by ^1H and ^{19}F NMR (Figure 1). The leftover acidic F_2B-OAc can then strongly bind to the OAc ligand on the allyliodonium intermediate **Int0**, thus leading to the key **Int1** species formulated as [PhI-(allyl)][$(OAc)_2BF_2$]. As expected, the allyl transfer stage is highly exergonic, especially once the latter O··B acid-base interaction is taken into account (ΔG = -50 kcal·mol^{-1} (see Figure S1). The equilibrium constant for the dissociation of **Int1** into the allyliodonium intermediate **Int1'** and $(OAc)_2BF_2$- anion, computed under simulated experimental conditions, showed that although the "naked" cationic **Int1'** constitutes the major component, a non-negligible proportion of the anion-bound λ^3-iodane **Int1** would also be present in solution (see Table S1).

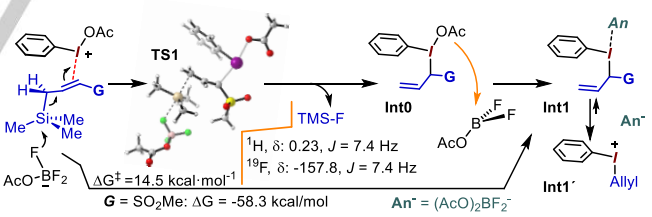

Figure 1. Simplified sequence (DFfT) for Si-to-I allyl transfer (G = SO_2Me).

In line with the iodonium-Claisen mechanism,[7] the carbon-carbon bond-forming step from both **Int1** and **Int1'** could take place via a readily accessible cyclic transition state. For the cationic **Int1'**, the rearrangement takes place with a $\Delta G^{\ddagger}$ energy of 11.9 kcal·mol^{-1} and leads to the Wheland-type intermediate **Int2'** located some 2.5 kcal·mol^{-1} lower than **Int1'** (Figure 2-top, G = SO_2Me, blue trace). The process is completed by a rapid proton transfer to the $(AcO)_2BF_2$ anion giving the final aromatic target. While a similar activation barrier was obtained for the unsubstituted system (G = H), the rearrangement stage in this case was thermodynamically uphill (Figure 2-top, red trace). It should be noted that although the chair conformation was used as the default geometry for the 6-membered **TS2'**, its boat-shaped counterpart (**TS2'**-boat**)** lies just ca. 2 kcal mol^{-1} higher in energy

10.1002/anie.202009369

(see Figure S2 in the ESI), suggesting that both paths are accessible. This study also provides one of the first detailed looks at the key cyclic transition state in an iodonio-Claisen process. Thus, analysis of **TS2'** revealed a significant synchronicity (Sy) value of 0.83, as well as the diatropic induced ring currents (Figure 2-bottom, left). In addition, calculations revealed considerable negative NICS(0)$_{zz}$ and NICS(1)$_{zz}$ values, as well the electron delocalization in the iodine-containing six-membered ring (Figure 2-bottom, right; see Fig. S9 for more details), all of which are consistent with non-negligible in-plane aromatic character of the transition state,[23] as would be expected for a thermally allowed pericyclic reaction (see Figure S3).

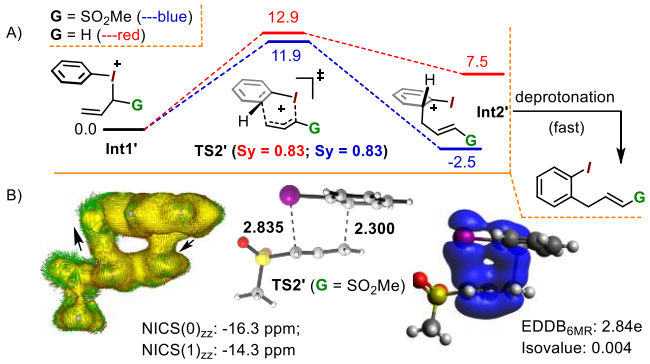

Figure 2. Top: DFT-based details of the key "iodo-Claisen" rearrangement step. Bottom: anisotropy of induced ring current density (ACID) plot (isovalue: 0.020 a.u.), key distances (Å), nuclear-independent chemical shift (NICS) values, and electron density of delocalized bonds (EDDB) in iodine-containing 6MR of **TS2'** (G = SO_2Me). ACID plots with higher resolution are given in the ESI.

Interestingly, for the non-dissociated **Int1** form, a concerted "all-in-one" stage was identified in which the rearrangement takes place with a simultaneous intramolecular H-removal by an O-atom of the bound anion, leading directly the aromatized product (see ESI, Figure S5). This process takes place with a higher $\Delta G^{\ddagger}$ = 14.1 kcal·mol^{-1}, while the barrier for the corresponding unsubstituted analogue (G = H) has the Gibbs energy barrier of 16.4 kcal·mol^{-1}. A lower Sy value of 0.49 is observed for this anion-assisted process. A priori, both the equilibrium constant and the activation energies favor the stepwise path taking place via cationic **Int1'**, as depicted in Figure 2. A similar preference was found for the analogues with G = SO_2Me and COOMe (see ESI). The lower Gibbs energy barriers associated to substrates with G = EWG (as compared to G = H) appear to stem from unequal destabilization effects caused by these substituents in the positively charged charge-localized **Int1'** and the more charge-delocalized **TS2'** (see NPA charges Table S2 of the ESI). An interesting aspect of the reaction is the apparent retention of the *trans* geometry of the *trans*-allylsilanes used throughout this work. A detailed look at the Si-to-I allyl transfer, already illustrated for the *trans* substrate in Figure 1, shows that the analogous transfer from a *cis* substrate takes place with a similar Gibbs energy barrier of 14.6 kcal mol^{-1}. Notably, the *cis*/*trans* stereo-information of the precursor would be lost, as both stereoisomers provide the same allyliodonium intermediate **Int1'**. Indeed, rather than being stereo-retentive, the *trans* outcome then arises from the stereo-preference in the rearrangements step. Specifically, two reactive dispositions of **Int1'** were identified, differing in their orientation of the SO_2Me moiety with respect to the ArI unit: the SO_2Me-**out** form (already shown in Figure 2), and the SO_2Me-**in** form for which the SO_2Me substituent points towards the aromatic core. As shown in Figure 3-A, while the **out**-form evolves to the *trans* product, the SO_2Me-**in** form would lead to the *cis* isomer. The *trans* selectivity would then stem from the $\Delta G^{\ddagger}$ energy for *cis* path being 1.8 kcal·mol^{-1} higher than for the *trans* path. The *trans* product should, therefore, be favored regardless of the initial allylsilane configuration, which leaves the door open to synthetically attractive stereo-convergent applications of *cis*/*trans* allylsilane mixtures. This was indeed confirmed via a selective conversion of *cis*-**6** to *trans*-**12** in 86% (Figure 3-B). This *trans* outcome, however, is only a *preference*, and so the cyclic allylsilane **57**, with a *cis*-locked CH_2Si / EWG pair, coupled readily with $PhI(OAc)_2$ to give **58** in 60% yield (9:1 *o/p*, Figure 3-C).

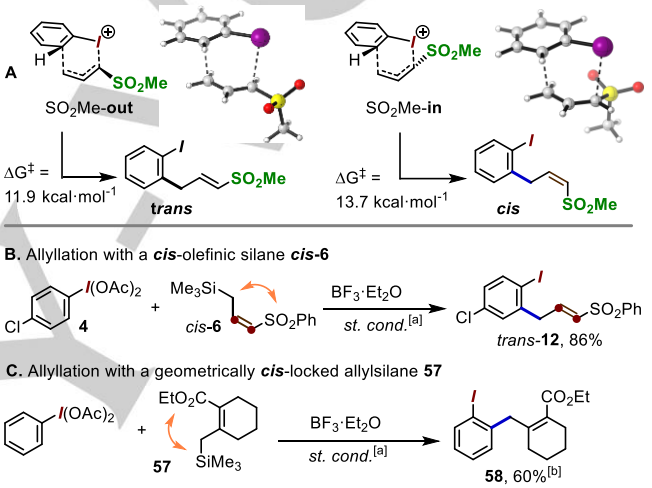

Figure 3. Insights into the stereoselectivity of the C-H allylation. **A**: Comparison between the computed *trans*- and *cis*-forming transition states. [a] Conditions as in Table 2; [b] 9:1 *ortho-para* regioisomeric ratio.

We also addressed the question of the high regio-preference of the 2-iodonapthalene core towards the C1-allylated products (e.g. **36** in Table 3). Hence, starting with a common λ^3-(2-naphthyl)allyliodonium intermediate, the activation barrier leading to the C1 product ($\Delta G^{\ddagger}$ = 6.6 kcal·mol^{-1}) was found to be 2.1 kcal·mol^{-1} lower than for the (unobserved) C3 path ($\Delta G^{\ddagger}$ = 8.7 kcal·mol^{-1}, see Fig. S7 of the ESI).

In terms of scope, a remarkable aspect of this C-H allylation reaction is the striking efficiency enhancement provided by electron-poor allylsilanes (G = EWG). Our results are consistent with the parent allyltrimethylsilane **1** evolving preferably through an umpolung process due to an attack of the ambient nucleophiles upon the highly electrophilic λ^3-allyl iodonium intermediate.[13a,11] This process, which can take place either through direct nucleophilic attack (e.g. via S_N2'), or via an S_N1 mechanisms, would compete with the productive rearrangement path (see Scheme 2-A).[15] Indeed, the reaction between allyltrimethylsilane (**1**) and the *p*-Cl λ^3-iodane **4** showed a nearly quantitative reduction of the hypervalent precursor to the *para*-chloro-iodobenzene, accompanied by a series of allylsilane umpolung byproducts, with the Ritter-derived *N*-allylacetamide as the major component in CH_3CN-containing solvent mixtures (Scheme 2-B; also see ESI). Our DFT calculations show that both

10.1002/anie.202009369
WILEY-VCH

RESEARCH ARTICLE

the S_N1 and S_N2' umpolung paths are energetically accessible, albeit with generally lower $\Delta G^{\ddagger}$ barrier in the S_N1 manifold.

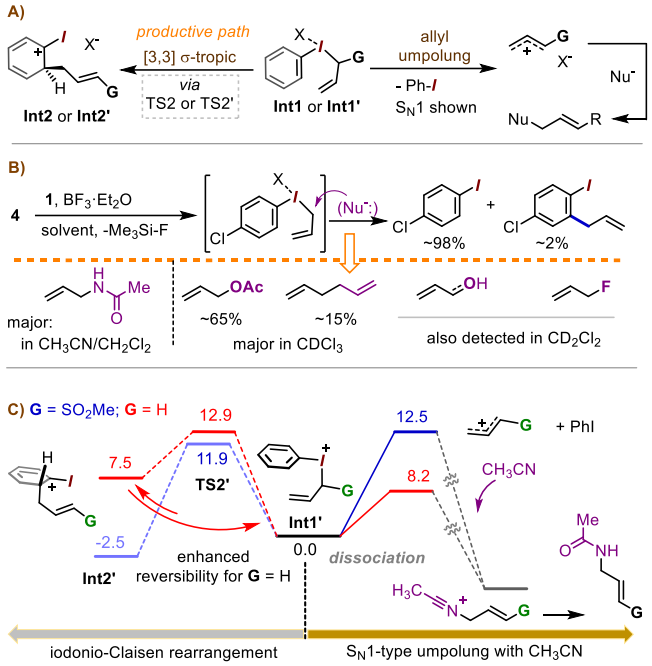

Scheme 2. Assessment of the allyl umpolung process in the context of the iodane-directed C-H allylation. B) observed umpolung products generated by a reaction of **4** with allylsilane **1**. C) a comparative profile in the evolution of **Int1'**.

Specifically, insights can be gained by comparing the overall energetic barriers between the target rearrangement and the umpolung process, e.g. S_N1 (Scheme 2-C). Despite the difficulty inherent in comparing intra- and intermolecular processes, our data suggest that the sulfonyl system (G = SO_2Me) favors the rearrangement path, with the $\Delta G^{\ddagger}$ = 11.9 kcal·mol^{-1} for rearrangement *vs* 12.5 kcal·mol^{-1} for S_N1. In contrast, the unsubstituted system (G = H) favors the S_N1 umpolung process by a $\Delta\Delta G^{\ddagger}$ of 4.7 kcal·mol^{-1} (see Figure S6 in the ESI). Furthermore, the exergonic nature of the rearrangement step for G = H (red trace, Figure 2) implies an iodonio-Claisen equilibrium favoring the **Int1'**, and, by extension, the likelihood of the competing umpolung reaction.

The amide challenge and downstream outlook. Wondering whether the allylsilane EWG requisites might be relaxed by the appropriate choice of conditions, we took a second look at the formation of amide-substituted allylarenes such as **47'** (Table 3), which had proven difficult with electron-deficient iodoarenes (also see last entries in Table 2). Interestingly, for such borderline cases, the use of 1,1,1,3,3,3-hexafluoro-isopropanol (HFIP) in combination with $BF_3{\cdot}Et_2O$ causes a drastic efficiency improvement, with the yield of **47'** going from the previously obtained 7% to 83% under the new conditions (Scheme 3-top). Importantly, poor results were obtained when omitting the BF_3 additive. Even the primary amide **10**, inefficient under standard conditions (see Table 1), now provided synthetically meaningful yields with both $PhI(OAc)_2$ and the *para*-Cl iodane **4** (Scheme 3-bottom, **59** and **60**). The mechanistic origin and the full synthetic potential of this medium are currently under study.

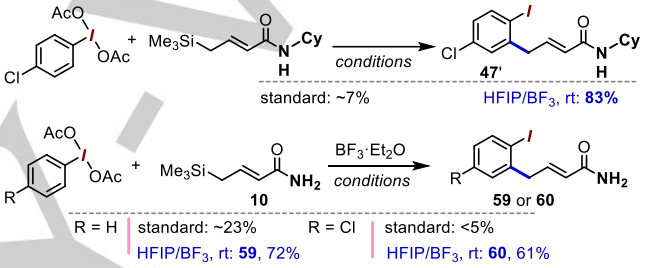

Scheme 3. Alternative conditions for amide-substituted allylsilanes.

The newly introduced allyl group could also be further elaborated, with applications including the formation of the alkenyl carbamate **61** (82%) (Scheme 4A), the Horner-Wadsworth-Emmons olefination to give polyenes such as the diene **SI-3** (ESI) or the triene **62** (Scheme 4B), or the conversion of the Weinreb amide **56** to the allyl ketone **SI-2** (see ESI). In another experiment, the crude allyliodane **17** was converted to the versatile vinyl diazoacetate **63** (Scheme 4C),[24] which underwent a thermally induced electrocyclization to give the 5-(2-iodophenyl)-1H-pyrazole **64** in 88% yield.

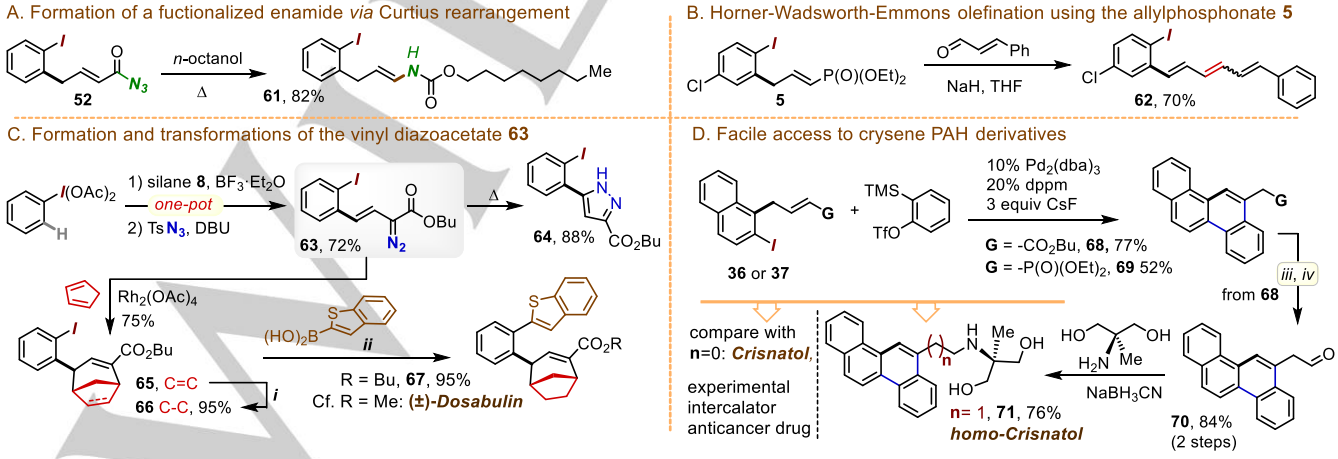

Scheme 4. Structural diversification based on the iodane-guided C-H allylation. Part C: *i*) $H_2NNH_2{\cdot}H_2O$, 10 mol% $CuCl_2$, air; *ii*) 5 mol% $Pd(PPh_3)_4$, Na_2CO_3, dioxane, 120 °C; part D: *iii*) $LiAlH_4$, THF, 0 °C to reflux; *iv*) $PhI(OAc)_2$, 10 mol% TEMPO, CH_2Cl_2. For details, see Electronic Supporting Information.

Motivated by a recent report on the usage the bromo-analogue of **63** as linchpin in a diversity-oriented medicinal chemistry project, the iodoarene **63** was applied to the ready synthesis of the *n*-Bu ester of (±)-Dosabulin, a potent antimitotic agent,[25] by exploiting the Rh-catalyzed cyclopropanation/ring expansion/reduction sequence to give **66** (via olefin **65**, Scheme 4C).[25] Thanks to the more reactive *ortho*-iodide, the yield in the final Suzuki-Miyaura step to give **67** improved from the original 78% to nearly quantitative.

In another extension, we envisaged accessing larger polycyclic aromatic hydrocarbons (PAH) via Pd-catalyzed formal [4+2] cycloaddition reaction developed by Worlikar and Larock.[26] Indeed, the Pd/dppm-catalyzed annulation of the iodonaphthalenes **36** or **37** with in-situ generated benzyne delivered the chrysene cores **68** and **69** in 77% and 52% yield, respectively (Scheme 4D). The usefulness of this transformation was highlighted by the ready conversion of the ester **68** to the aminoalcohol **71** (via aldehyde **70**), a one-carbon homologue of the intercalator-type experimental anticancer agent Crisnatol.[27] We note that our primary aim with sequences such as **C** and **D** in Scheme 4 is not necessarily to improve upon existing routes, but rather to highlight the potential of the iodane-guided C-H allylation as a tool to rapidly scan swaths of chemical space of interest.

Conclusion

In summary, functionalized *ortho*-allylated iodoarenes can be obtained by iodane-guided C-H functionalization. In this process, the efficiency of the C-H allylation is unlocked through to the introduction of a terminal EWG groups to the allylsilane, including the SO_2R, the -$PO(Et)_2$ or a variety of –COX substituents. Such substrates were conveniently accessed through olefin cross-metathesis, including a modular variant involving acryloyl chloride. The method could be applied to a series of activated and deactivated iodoarenes cores. DFT calculations revealed that, after a low-barrier Si-to-I allyl transfer, in the case of EWG-substituted allylsilanes a [3,3] sigmatropic rearrangement takes place through an aromatic transition state to yield *ortho*-allylated iodoarenes, whereas for unsubstituted allylsilane the S_N1 umpolung process is preferred for non-activated iodoarene cores. The newly prepared *o*-iodo allylarenes constitute a valuable family of building blocks, as was illustrated by applications ranging from the double bond migration and HWE olefination, to the synthesis of cores based on the experimental agents Dosabulin and Crisnatol. We feel that these applications are but a tip of the iceberg, and that many more uses for the functionalized iodoarenes produced by this method will be discovered.

Acknowledgements

This work was funded by MINECO (CTQ2017-86936-P, CTQ2017-85341-P) and AGAUR (2017 SGR 01051, 2017 SGR 00294, 2017 SGR 00039). Financial support from CSIC, URL (2019-URL_Proj-034) and IQS-Obra Social La Caixa (2017-URL-Intermac-010) is also gratefully acknowledged. The State Scholarship Fund (No. 201906310040, D.C.) from the China Scholarship Council (CSC), the National Science Foundation of China (21573179, J.Z.), the Top-Notch Young Talents Program of China (J.Z.) are also gratefully acknowledged.

Keywords: C-H functionalization • C-C coupling • hypervalent iodine • allylation • arenes

[1] For an unavoidably incomplete selection, see the following reviews and references therein a) J. D. Weaver, A. Recio, A. J. Grenning, J. A. Tunge, *Chem. Rev*. **2011**, *111*, 1846−1913; b) M. Yus, J. C. González-Gómez, F. Foubelo, *Chem. Rev*. **2011**, *111*, 7774−7854; c) Z. Lu, S. Ma, *Angew. Chem. Int. Ed*. **2008**, *47*, 258−297.

[2] For example, see: a) J. L. Farmer, H. N. Hunter, M. G. Organ, *J. Am. Chem. Soc.* **2012**, *134*, 17470−17473.

[3] For selected examples of the metal-catalyzed C(sp^2)-allylation with allylstannanes, see: a) A. M. Echavarren, J. K. Stille, *J. Am. Chem. Soc*. **1987**, *109*, 5478−86; b) V. Farina, B. Krishnan, *J. Am. Chem. Soc*. **1991**, *113*, 9585−9595; c) M. Pérez-Rodríguez, A. A. C. Braga, A. R. de Lera, F. Maseras, R. Álvarez, P. Espinet, *Organometallics* **2010**, *29*, 4983−4991; for a recent review, see: d) C. Cordovilla, C. Bartolomé, J. M. Martínez-Ilarduya, P. Espinet, *ACS Catal.* **2015**, *55*, 3040−3053; for a multi-gram application, see: e) M. J. Zacuto, C. S. Shultz, M. Journet, *Org. Proc. Res. Dev*. **2011**, *15*, 158−161.

[4] For regiochemistry control, see: Y. Yang, S. L. Buchwald, *J. Am. Chem. Soc.* **2013**, *135*, 10642−10645.

[5] For a recent review on catalytic C_{sp2}-H allylation, see: a) N. K. Mishra, S. Sharma, J. Park, S. Han, I. S. Kim, *ACS Catal.* **2017**, *7*, 2821−2847. Also, see b) H. Wang, N. Schröder, F. Glorius, *Angew. Chem. Int. Ed*. **2013**, *52*, 5386−5389 and references therein.

[6] For general information on hypervalent iodine reagents see: a) A. Yoshimura, V. V. Zhdankin, *Chem. Rev*. **2016**, *116*, 3328−3435; b) *Hypervalent Iodine Chemistry. Modern Developments in Organic Synthesis,* Editor: T. Wirth, Springer 2003; c) F. V. Singh, T. Wirth, *Chem. Asian J.* **2014**, *9*, 950−971; d) L. F. Silva, B. Olofsson, *Nat. Prod. Rep.* **2014**, *28*, 1722−1754; e) PATAI'S Chemistry of Functional Groups, Ed. B. Olofsson, I. Marek, Z. Rappoport, John Wiley & Sons, Ltd, Chichester, UK, 2019.

[7] a) M. Ochiai, T. Ito, Y. Takaoka, Y. Masaki, *J. Am. Chem. Soc.* **1991**, *113*, 1319−1323; b) D. A. Gately, T. A. Luther, J. R. Norton, M. M. Miller, O. P. Anderson, *J. Org. Chem.* **1992**, *57*, 6496−6502.

[8] S. Izquierdo, S. Bouvet, Y. Wu, S. Molina, A. Shafir, *Chem. Eur. J*. **2018**, *24*, 15517−15521.

[9] For the iodane-guided coupling with enols and phenols, see: a) Z. Jia, E. Gálvez, R. M. Sebastián, R. Pleixats, A. Álvarez-Larena, E. Martin, A. Vallribera, A. Shafir, *Angew. Chem. Int. Ed*. **2014**, *53*, 11298−11301; b) Y. Wu, I. Arenas, L. M. Broomfield, E. Martin, A. Shafir, *Chem. Eur. J.* **2015**, *21*, 18779−18784; c) M. Hori, J.-D. Guo, T. Yanagi, K. Nogi, T. Sasamori, H. Yorimitsu, *Angew. Chem. Int. Ed*. **2018**, *57*, 4663−4667; d) X. Huang, Y. Zhang, C. Zhang, L. Zhang, Y. Xu, L. Kong, Z.-X. Wang, B. Peng, *Angew. Chem. Int. Ed.* **2019**, *58*, 5956−5961; for *ortho*-cyanoalkylation, see: e) J. Tian, F. Luo, C. Zhang, X. Huang, Y. Zhang, L. Zhang, L. Kong, X. Hu, Z.-X. Wang, B. Peng, *Angew. Chem. Int. Ed.* **2018**, *57*, 9078−9082.

[10] C. Mowdawalla, F. Ahmed, T. Li, K. Pham, L. Dave, G. Kim, I. F. D. Hyatt, *Beilstein J. Org. Chem.* **2018,** *14,* 1039−1045.

[11] Y. Wu, S. Bouvet, S. Izquierdo, A. Shafir, *Angew. Chem. Int. Ed*. **2019**, *58*, 2617−2621.

[12] For recent reviews, see: a) G. Grelier, B. Darses, P. Dauban, *Beilstein J. Org. Chem.* **2018,** *14,* 1508−1528; b) A. Boelke, P. Finkbeiner, B. J. Nachtsheim, *Beilstein J. Org. Chem.* **2018,** *14,* 1263−1280; c) I. F. D. Hyatt, L. Dave, N. David, K. Kaur, M. Medard, C. Mowdawalla, *Org. Biomol. Chem.* **2019**, *17*, 7822.

[13] a) H. R. Khatri, J. Zhu, *Chem. Eur. J*. **2012**, *18*, 12232−12236; b) H. Nguyen, H. R. Khatri, J. Zhu, *Tetrahedron Lett*. **2013**, *54*, 5464−5466; c) H. R. Khatri, H. Nguyen, J. K. Dunaway, J. Zhu, *Front. Chem. Sci. Eng*. **2015**, *9*, 359−368; also see: d) K. L. Dae, Y. K. Dong, Y. Oh, *Tetrahedron Lett*. **1988**, *29*, 667−668.

[14] For related sulfoxide-guided reactivity, including *ortho*-allylation see: a) A. J. Eberhart, J. E. Imbriglio, D. J. Procter, *Org. Lett*. **2011**, *13*, 5882−5885; b) H. J. Shrives, J. A. Fernandez-Salas, C. Hedtke, A. P. Pulis, D. J. Procter, *Nat. Commun*. **2017**, *8*, 14801; c) X. Huang, M. Patil, C. Farès, W. Thiel, N. Maulide, *J. Am. Chem. Soc*. **2013**, *135*, 7312−7323.

[15] a) T. Okuyama, T. Takino, T. Sueda, M. Ochiai, *J. Am. Chem. Soc*. **1995**, *117*, 3360-3367; also see: b) M. Ochiai, M. Kida, T. Okuyama, *Tetrahedron Lett*. **1998**, *39*, 6207−6210.

[16] For focus reviews on iodane-guided C-H coupling, see: a) A. Shafir, *Tetrahedron Lett.* **2016**, *57*, 2673−2682; b) W. W. Chen, A. B. Cuenca, A. Shafir, *Angew. Chem. Int. Ed*. **2019**, doi.org/10.1002/anie.201908418; also, see: b) S. E. Wengryniuk, S. Canesi, *Rearrangements and Fragmentations Mediated by Hypervalent Iodine Reagents*, in PATAI'S Chemistry of Functional Groups, John Wiley & Sons, Ltd, Chichester, UK, 2019, pp. 1−41.

[17] A. K. Chatterjee, T.-L. Choi, R. H. Grubbs, *Synlett* **2001**, 1034−1037.

[18] For details on the activation of $ArI(OAc)_2$ with BF_3, see: S. Izquierdo, S. Essafi, I. del Rosal, P. Vidossich, R. Pleixats, A. Vallribera, G. Ujaque, A. Lledós, A. Shafir, *J. Am. Chem. Soc*. **2016**, *138*, 12747−12750.

[19] See Scheme 2 for a more detailed picture of this failed process.

[20] Electronic parameters as collected in C. Hansch, R. Leo, R. W. Taft, *Chem. Rev*.**1991**, *91*, 165−195.

[21] a) A. S. Radhakrishna, M. E. Parham, R. M. Riggs, G. M. Loudon, *J. Org. Chem.* **1979**, *44*, 1746-1747; b) R. M. Moriarty, C. J. Chany II, R. K. Vaid, O. Prakash, S. M. Tuladhar, *J. Org. Chem*. **1993**, *58*, 2478– 2482; c) A. A. Zagulyaeva, C. T. Banek, M. S. Yusubov, V. V. Zhdankin, *Org. Lett.* **2010**, *12*, 4644-4647; d) A. Yoshimura, K. R. Middleton, M. W. Luedtke, C. Zhu, V. V. Zhdankin, *J. Org. Chem*. **2012**, *77*, 11399−11404; e) K. Miyamoto, Y. Sakai, S. Goda, M. Ochiai, *Chem. Commun*. **2012**, *48*, 982−984.

[22] L. Ferrié, S. Bouzbouz, J. Cossy, *Org. Lett.*, **2009**, *11*, 5446−5448.

[23] P. v. R. Schleyer, J. I. Wu, F. P. Cossío, I. Fernández, *Chem. Soc. Rev*. **2014**, *43*, 4909—4921.

[24] H. M. L. Davies, T. J. Clark, H. D. Smith, *J. Org. Chem.* **1991**, *56*, 3817−3824.

[25] B. M. Ibbeson, L. Laraia, E. Alza, C. J. O'Connor, Y. S. Tan, H. M. L. Davies, G. McKenzie, A. R. Venkitaraman, Spring, D. R. *Nat. Commun*. **2014**, *5*, 3155.

[26] a) S. A. Worlikar, R. C. Larock, *Org. Lett*. **2009**, *11*, 2413−2416.

[27] a) K. W. Bair, R. L. Tuttle, V. C. Knick, M. Cory, D. D. McKee, *J. Med. Chem*. **1990**, *33*, 2385−2393; b) K. W. Bair, US4719046A (1984).

10.1002/anie.202009369

WILEY-VCH

RESEARCH ARTICLE

Entry for the Table of Contents

Insert graphic for Table of Contents here.

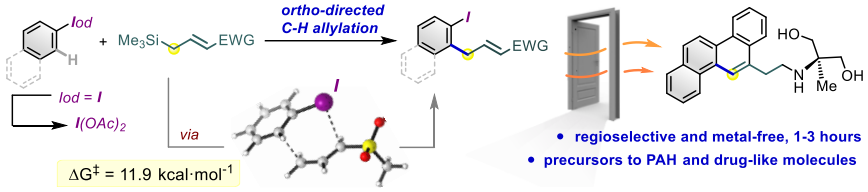

Metal-free C-H allylation is described to access a wide range of functionalized *ortho*-allyl-iodoarenes. The method employs (diacetoxy)iodoarene precursors and proceeds through the iodane-guided “iodonio-Claisen” allyl transfer. The method is based on the usage of allylsilanes bearing electron-withdrawing groups and is compatible with an electronically broad range of iodoarenes. DFT calculations support the reaction taking place through an in-plane aromatic cyclic transition state, and suggest that the EWG substituents help discourage the competing umpolung oxidation of the allylic precursor. The resulting *ortho*-allylated iodoarenes are versatile building blocks, with examples of downstream transformation including a concise synthesis of core of the experimental antimitotic agent Dosabulin.